Characterization of Sc/Mg multilayers with and without Co barriers layers for x-ray spectroscopy in the water window range

Philippe Jonnard, Meiyi Wu, Karine Le Guen, Angelo Giglia, Konstantin Koshmak, Qiushi Huang, Zhe Zhang, Zhanshan Wang, Imene Esteve, Nicolas Menguy, et al.

Characterization of Sc/Mg multilayers with and without Co barriers layers for x-ray spectroscopy in the water window range

Philippe Jonnard[a,1], Meiyi Wu[a,*], Karine Le Guen[a], Angelo Giglia[b], Konstantin Koshmak[b], Qiushi Huang[c], Zhe Zhang[c], Zhanshan Wang[c], Imène Estève[d], Nicolas Menguy[d], Béatrice Doisneau[d]

[a] Sorbonne Université, Faculté des Sciences et Ingéniérie, UMR CNRS, Laboratoire de Chimie Physique-Matière et Rayonnement, 4 place Jussieu, F-75252 Paris cedex 05, France

[b] CNR-IOM Laboratorio TASC, Basovizza SS-14, km 163.5, I-34012 Trieste, Italy

[c] Key Laboratory of Advanced Micro-Structured Materials MOE, Institute of Precision Optical Engineering, School of Physics Science and Engineering, Tongji University, Shanghai 200092, China

[d] Sorbonne Université, UMR CNRS 7590, Muséum National d'Histoire Naturelle, Institut de Minéralogie, de Physique des Matériaux et de Cosmochimie (IMPMC), 4 place Jussieu, F-75005 Paris, France

* On leave to IMEC, Leuven, Belgium

Abstract

We characterize nano-scale periodic Sc/Mg two-layer, Sc/Mg/Co tri-layers and Sc/Co/Mg/Co quadri-layer designed as dispersive elements for x-ray spectroscopy in the nitrogen K range (390 eV). The samples are prepared by magnetron sputtering with Mg and Sc layers being a few nanometers thick and Co layers being of sub-nanometric thickness. We apply non-destructive (x-ray reflectivity and x-ray fluorescence in standing wave mode) and destructive (transmission electron microscopy) techniques to obtain a relevant description of the deposited stacks. It turns out that a strong interdiffusion takes place in the two-layer leading to poor reflective properties. Interdiffusion also occurs in the tri-layers and quadri-layer but between the Sc and Co layers. These systems can be considered as periodic ScCo/Mg two-layers with well-defined layers. As a consequence, the Sc/Co/Mg/Co multilayer is found interesting to use for spectroscopy as a reflectance of 32% is expected in the N K range in the water window range.

Keywords: periodic multilayer; Mg; Sc; Co; interface

[1] Corresponding author : philippe.jonnard@sorbonne-universite.fr

Introduction

Periodic multilayers made of an alternation of two or more thin films of nano-scale thickness are important optical elements for the x-ray range [1]. Indeed, as their period ranges from a few nm to some tens of nm, they can diffract x-ray radiation whose wavelength ranges from 0.1 to 10 nm. Within this range, the so-called water-window range, located between the absorption edges of carbon (285 eV) and oxygen (530 eV), is particularly interesting as it is possible to image biological samples with a good contrast and also owing to the presence of the nitrogen K absorption edge (395 eV) and Kα characteristic emission (393 eV) [2].

For imaging purpose at near-normal incidence, the Cr/Sc system [3,4], with or without thin diffusion barrier layers, as well as other systems [5–8], have been developed. We are here interested for the spectroscopic purpose in the range of the nitrogen K emission band. Indeed, no crystal can operate in this range owing to the long wavelength to disperse. Thus, such spectroscopy requires the use of a grating spectrometer [9] or of a crystal spectrometer equipped with a suitable periodic multilayer [10–13]. However, the low fluorescence yield of nitrogen combined to the low reflectance of grating and multilayers makes the study of this spectral range difficult. In the case of crystal spectrometer, any multilayer, which could present a high reflectance at the rather small glancing angle required for x-ray spectroscopy, is welcome.

In this framework, we study the Sc/Mg system. Indeed, simulations with a perfect (without roughness or interdiffusion) periodic multilayer of 6 nm period, having 40 bilayers, show that a reflectance higher than 62% can be expected for a glancing angle close to 15° and a photon energy slightly lower than the N K edge, where is present the N Kα emission. This reflectance value is slightly higher than what can be expected from the standard Sc/Cr multilayer commonly used in this photon energy range. The Sc/Mg system can also provide a better spectral resolution as its bandwidth is around 5 eV while that of Sc/Cr is 6 eV. However, because some interdiffusion can develop between the Sc and Mg layers, we also consider Sc/Co/Mg tri-layers with different orders of the layers and the Sc/Co/Mg/Co quadri-layer. Thin layers of Co has been chosen as a diffusion barrier as we know that the Mg/Co system presents sharp interfaces [14].

The characterization of the samples was made by using non-destructive techniques, hard x-ray reflectivity as well in the soft x-ray range close to the Mg K absorption edge and x-ray fluorescence in x-ray standing wave condition [15,16] and a destructive one, transmission electron microscopy on cross section. The reflectivity measurements allow obtaining a first description of the structural parameters, thickness, roughness and density of the layers, of a periodic stack. In x-ray standing wave mode, the angular distributions of the intensity of the characteristic emissions, when scanned around the Bragg angle, depend on the elemental depth distributions. In electron microscopy, cross sections first prepared by focused ion beam, were observed at ultra-high resolution and in high-angle annular dark-field imaging mode. This was completed by elemental depth profiles obtained from elemental x-ray fluorescence maps.

Experimental details

Sample preparation

The samples were prepared by direct current magnetron sputtering. The base pressure in the deposition chamber was 6.0×10^{-5} Pa. High purity argon (99.999%) was used as the sputtering gas at a pressure of 0.13 Pa. The depositions rates of Mg, Sc and Co were approximately 0.35, 0.07 and 0.11 nm/s, respectively.

The following samples were deposited on polished Si (100) wafers:

#1. B_4C (3nm) / [Sc(3nm)/Mg (3nm)]x40 / Co (4nm) / Si substrate

#2. B_4C (3nm) / [Sc(3nm)/Co(0.45nm)/Mg(3nm)]x40 / Co (4nm) / Si substrate

#3. B_4C (3nm) / [Sc(3nm)/Mg(3nm)/Co(0.45nm)]x40 / Co (4nm) / Si substrate

#4. B_4C (3nm) / [Co(0.45nm)/Sc(3nm)/Co(0.45nm)/Mg(3nm)]x40 / Co (4nm) / Si substrate.

They consist of one two-layer (#1), two tri-layers with Co layers either at the Sc-on-Mg (#2) or Mg-on-Sc (#3) interfaces and a quadri-layer (#4) with Co layers at both Sc-on-Mg and Mg-on-Sc interfaces. The thickness of the cobalt interlayer has been chosen to 0.45 nm, thick enough to prevent interdiffusion between Co and Mg. A thin cobalt layer has been deposited between the substrate and the stack to improve adhesion. The superficial capping B_4C layer is to protect the stack from oxidation.

Just after their preparation, the samples were characterized by x-ray reflectivity at 0.154 nm, see figure 1. From a qualitative point of view, only one Bragg peak is seen for the two-layer, up to three for the tri-layers and five for the quadri-layer. This clearly indicates that the two-layer does not provide a good reflectivity and that the quality of the multilayer improves with the number of Co barrier layers in the stack. If descriptions of the stacks without the formation of new interlayer are considered to fit the reflectivity curves, then the thicknesses of the layers are found close to the designed ones. In this condition, the interfacial width range between 0.4 and 0.9 nm.

Figure 1: X-ray reflectivity at 0.154 nm measured on the four studied periodic multilayers. The curves are shifted vertically for sake of clarity.

Reflectivity in the soft x-ray range

Measurements were made at the BEAR beamline of the Elettra synchrotron [17]. The incident beam size was 400 µm × 50 µm, vertical × horizontal. Incoming and reflected intensities were measured with a SXUV 100 photodiode during an integration time of 0.5 s. Reflectance was measured in the range of the Mg K absorption edge at 1300.5 eV, where high reflectance is expected. First measurement was performed as a function of the incident photon energy at a given angle to determine the energy of the maximum of the reflectivity curve. Then, reflectance was measured at this energy as a function of the glancing angle in θ-2 θ mode. The simulations of reflectivity curves have been done using the IMD software [18].

X-ray fluorescence in x-ray standing wave condition

X-ray fluorescence was measured in the same experimental end station as soft-ray reflectance. A silicon drift detector, with a resolution better than 150 eV at 5.9 keV, was used

to detect the characteristic emissions of the samples. There is a fixed angle of 60° between the incident photon beam and the direction of detection.

To perform these measurements in the x-ray standing wave mode, fluorescence spectra were collected for a numerous number of angles spanning the Bragg angle, the angle fulfilling the Bragg law with the multilayer period and the incident photon energy. The photon energy was chosen as 1300.5 eV, obtained experimentally from an x-ray absorption measurement in the Mg K edge. This photon energy corresponds to the first half of the absorption jump, so that it is possible to generate Mg 1s core holes, while still presenting a high reflectance, enabling the generation of well-contrasted standing waves. In this condition, both Mg Kα and Co Lαβ emissions can be generated (scandium Lαβ mission is at a too low energy to be efficiently detected). The intensity under the Mg Kα and Co Lαβ peaks is plotted as a function of the glancing angle to obtain the x-ray standing wave curves.

These curves were simulated by a model [19,20] relying on the recursive method to calculate the depth distribution of the electric field of the incident radiation, and on the reciprocity theorem to calculate the distribution of the electric field of the emitted radiation. For comparison with the experiments, the simulations were divided by a geometrical factor [21] taken as a sine function. Then, they were convolved by a rectangular function to take into account the angular divergence of the incident beam.

Scanning transmission electron microscopy

Only the two-layer and quadri-layer samples were chosen for observation by transmission electron microscopy (TEM). First cross sections were prepared by focused ion beam (FIB) on a Zeiss Neon 40EsB equipment. Before milling, a platinum strap was deposited onto the region of interest of the sample. Then, the initial milling steps were operated with a Ga^+ beam at 30 kV and 2 nA, consisting in the rough excavation from both sides of the thin foil. Then, an *in situ* micromanipulator was used to weld the foil onto a copper grid. The thinning steps were performed with decreasing the current till the end with a 100 pA ion current on both sides of the foil in order to reach a thickness of about 55 nm.

The thin slabs were observed on a JEOL 2100F transmission electron microscope operating at 200 kV. The microscope is equipped with a field electron gun, an ultra-high resolution pole piece, a JEOL detector with an ultra-thin windowing detection of light elements and a scanning TEM (STEM) device. This last device allows Z-contrast imaging in high angle annular dark field mode (HAADF). Both ultra-high resolution (UHR, for the two- and quadri-layer samples) and HAADF (for the quadri-layer sample only) images in a scanning mode were obtained. Elemental mapping was acquired by energy dispersive x-ray spectrometry in the STEM mode, using the JEOL software Analysis Station. The HAADF images and elemental maps, obtained at the energies of the characteristic emissions of the elements present in the stack, were collected only for the quadri-layer. The maps were integrated perpendicularly to the stratification direction to obtain the corresponding elemental profiles.

Results and discussion

We show in figure 2 the reflectivity curves measured in the Mg K range. They are in line with the x-ray reflectivity curves obtained in the hard x-ray range. The two-layer presents

a poor reflectance. This demonstrates that the structure of this stack is still that of a periodic multilayer but however with structural parameters far from the designed ones. Both tri-layers present similar reflectance and bandwidth, however Sc/Mg/Co being a little better. The position of their maximum is shifted toward the low angles with respect to the two-layer. This shift is explained by the larger period of the stacks, owing to the introduction of the Co thin layers. The quadri-layer presents the highest reflectance. We note that its maximum lies between those of the two-layer and tri-layer in the Mg K range. However, from its design with the largest period, one would expect the quadri-layer to present the lowest angle of the maximum of the reflectivity curve. This means that large interdiffusion process takes places at interfaces, creating interlayers with different densities and thus different thicknesses. Interdiffusion processes are discussed below. All the stacks present reflectance quite far from the value expected for perfect multilayers. Thus, some interfacial processes are in play in these structures, which degrade their optical properties.

Figure 2: Reflectance of the four studied multilayers measured at a photon energy close to the Mg K edge (1300.5 eV).

We show in figure 3 the x-ray standing wave curves giving the angular distributions of the Co L and Mg K emissions of the samples, when irradiated at 1300.5 eV. They present two main regions: at low angles (1 – 2°) where total internal reflection occurs; at large angles (4 – 5°) where intensity is modulated owing to the formation of the standing waves when the Bragg condition is fulfilled for the incident radiation. It is seen on the Mg K curve that no feature appears in the Bragg region for the two-layer. This demonstrates, in agreement with the previous reflectivity measurements, that the periodicity of the stack is so bad and the optical contrast between layers so poor that it is not possible to generate strong constructive interferences and thus a well-contrasted standing wave field. Thus the Co L emission of the two-layer sample has not been measured. Also in agreement with the reflectivity measurements, both tri-layers give very similar curves. Again, the quadri-layer is found of better quality as its curves are better contrasted with respect to the ones of the tri-layers. This is particularly true for the Mg K emission. Finally, let us note that both tri-layers present the same total reflection angle, about 0.25° smaller than the one of the quadri-layer. As is well known, this angle is related to the mean density of the stack [1]. Thus, we can deduce that the quadri-layer has a mean density slightly higher than the tri-layers. This is very probably due to the formation of interlayers in the tri-layers that have a density lower than the mean of the densities of the individual layers.

Figure 3: X-ray standing wave curves of the Co L (a) and Mg K (b) emissions of the four studied samples excited by 1300.5 eV photons.

We show in figure 4 a transmission electron microscopy image of the cross section of the two-layer. On the image, the grey region on the upper left corner is the silicon substrate. Then, comes the thin cobalt adhesion layer observed as a black stripe. The multilayer follows, with on its top (on the right of the image) the bright boron carbide capping layer. The black region in the lower right corner is the Pt layer deposited onto the stack during the FIB process. It can be seen that close to the substrate the quality of the layers seems good but after of few

periods some degradation occurs, leading to some blurring or even disappearance of the layers and finally waviness at the top of the stack. These observations provide an explanation of the bad reflective properties of the bilayer system.

Figure 4: Transmission electron microscopy image of the whole two-layer. The silicon substrate is in the upper left corner.

We present in figures 5(a) and (b) for the quadri-layer, the HAADF image of the whole stack and a UHR image obtained close to the Si substrate, respectively. From the observation of the whole multilayer, it is clear that the stack is well periodic with well-contrasted layers, explaining the better optical performance of this system. The description of figure 5(a) from top to bottom is: silicon substrate observed as black; cobalt adhesion layer observed as a white stripe; multilayer; dark boron carbide capping layer; bright Pt layer. The period of the stack is measured as 6.6 ± 0.1 nm.

Figure 5: HAADF (a) and high-resolution (b) electron microscopy images of the quadri-layer. The contrast is reversed between the two images. (c) Profile of 5 periods obtained from a high magnification HAADF image.

What is striking from the observation of the multilayer is that it presents itself as a two-layer and not as a quadri-layer. HAADF images obtained at higher magnification did not allow showing additional layers. This is confirmed by the UHR image of figure 5(b). Only a two-layer is observed with crystallized bright layers. Figure 5(c) presents a profile of 5 periods of the stack, obtained from a HAADF image taken at high magnification. The bilayer structure is clearly observed. The zones of high intensity correspond to the mixed or unresolved Co/Sc/Co, noted ScCo, layers; the zones of low intensity to the Mg layers. The thicknesses of the Mg and ScCo layers, obtained by measuring the depth of the inflexion points on the profile and taking the mean of all the widths, are 2.7 and 3.9 ± 0.2 nm respectively. The profile of ScCo layers is clearly asymmetrical: the Co-on-Sc side is more diffuse than the Sc-on-Co side. This pattern is found everywhere in the prepared slab. The contrast of HAADF images being sensitive to the chemical state of the observed species, the observation of the asymmetry gives evidence of different mixings taking place at the Sc-on-Co and Co-on-Sc interfaces.

The bilayer structure of the quadri-layer stack is confirmed from the elemental depth profiles determined from the Co K, Mg K and Sc K elemental maps as shown in figure 6(b). These profiles clearly show that Mg and Sc are in phase opposition, Mg and Co are in phase opposition and Sc and Co are in phase. This demonstrates the positive effect of Co as a diffusion barrier between Mg and Sc. However, the thin Co layers are fully mixed (within the experimental resolution) with the Sc layers. A partial mixing would have been observed as a double peak in the Co profile, whose maxima would have been present at both sides of the Sc profile maxima. Here, for all the periods of the stack, both maxima of the Co and Sc profiles are located at the same depth. It is not possible with the given experimental uncertainty to see if there is some asymmetry of the interfaces, as deduced from the HAADF profile.

Figure 6: Elemental depth profiles of the quadri-layer obtained in the vicinity of the substrate (a), inside (b) and at the top of the stack (c).

The Si K, C K, O K and Pt M profiles were also obtained to determine what happens at both extremities of the quadri-layer. Toward the substrate, figure 6(a), there is no diffusion of silicon inside the stack, but a small amount of oxygen at the interface between Si and the Co adhesion layer owing to the presence of the Si native oxide. At the topmost surface, figure 6(c), the carbon from the boron carbide capping layer is mixed with the Pt layer (there are also some carbon atoms in the Pt precursor used to make the protective coating). We can see that the first Sc layer plays the role of barrier against the oxidation from the atmosphere instead of the boron carbide capping layer. This mixed layer of Sc and O is less dense than the mixed Sc and Co layers. This explains why on the HAADF image, figure 5(a), the first Sc layer is dark grey whereas the others are bright grey. After, these superficial layers, there is no more significant amount of oxygen present in the multilayer.

From the examination of the mixing enthalpies of the different elements, it is possible to understand why the quadri-layer turns into a bilayer. Indeed the maximum values of enthalpy, calculated from the semi-empirical Miedena model [22], for Mg-Co, Mg-Sc and Sc-Co are respectively +0.85, -5 and -30 kJ/mol. This means that Mg and Co cannot mix, and that Mg and Sc as well as Sc and Co can mix, but the mixing will be much easier between Sc and Co. Thus from this point of view, in the quadri-layer the Mg layers should remain free of Co and Sc atoms whereas Sc and Co layers should mix. Taking into account the number of deposited atoms, we expect the formation of a layer of $Co_{0.9}Sc_3$ composition, close to composition of the $CoSc_3$ compound found in the Sc-Co phase diagram [23].

The values of the mixing enthalpy also explain the bad quality of the Mg/Sc two-layer. Without diffusion barriers, the Mg and Sc layers can mix as soon as they are deposited. By analogy to what happens in the quadri-layer, we expect that the Sc and Co layers fully mix in the tri-layers to form a bilayer stack. In this case the composition of the mixed compound should be $Co_{0.45}Sc_3$. We expect the density of this compound to be lower than the one found in the quadri-layer. Thus, the mean density of the tri-layers is lower than that the quadri-layer. This result is consistent with the shift of the total reflection angle observed on the x-ray standing wave curves, figure 3.

We take into account the description gained from the electron microscopy observation and elemental maps to create a new description of the quadri-layer sample. We now consider the following stack, $B_4C/Sc_2O_3/Sc_3Co/Mg/[Sc_3Co/Mg]_{x39}/Co/Si$ substrate, to fit the reflectivity curves in the hard and soft x-ray ranges, figure 7(a) and 7(b) respectively. With respect to the design with 40 periods (given in the experimental section), here we consider that the first period is oxidized (Sc_2O_3) and mixed (Sc_3Co), after which 39 identical bilayers follow each other down to the bottom of the stack. A good fit is obtained in both ranges with the same parameters of the stack: thickness, roughness and density of the various layers. They are collated in Table 1. In this description, the period of the stack is 6.65 nm a little lower than the designed one, 6.9 nm, but in good agreement with the one measured on the HAADF image. The thicknesses of the two layers are also in agreement with the values obtained from the profile of the HAADF image, figure 5(c). The roughness of the ScCo and Mg layers in the periodic structure is limited below 0.8 nm. Thus the quadri-layer structure is made of well-defined layers and should be suitable to provide a high reflectance in the N K range. A simulation of the reflectivity curve in this

range, shown in figure 8, confirms this point. A reflectance value of 32% is reached at 398 eV and 13°, and should allow acquiring x-ray spectra in an efficient way.

Figure 7: Experimental (dots) and fitted (solid line) reflectivity curves of the quadri-layer sample in the hard x-ray (a, in log scale) and soft x-ray (b, in linear scale) ranges.

Table 1: Structural parameters of the layers used to describe the quadri-layer stack in order to fit the reflectivity curves presented in Figure 7. Layers are presented from the top to the bottom. Layers #2-4 represent the first period in the designed stack, oxidized and mixed. Layers #5-6, noted ML, are those present in the 39 periods of the considered stack. Density values in italics are those of the bulk materials.

	Layer	Thickness ±0.05 nm	Roughness ± 0.05 nm	Density ±0.5 g.cm^{-3}
#1	B_4C	1.44	0.21	*2.52*
#2	Sc_2O_3	1.58	0.23	3.4
#3	Sc_3Co	2.74	0.17	3.05
#4	Mg	1.75	0.23	*1.74*
#5	Sc_3Co ML	4.18	0.64	4.39
#6	Mg ML	2.47	0.67	*1.74*
#7	Co	1.25	0.76	*8.9*
#8	Si substrate	-	0.09	*2.33*

Figure 8: Reflectance calculated in the N K range (398 eV) of the multilayer stack described with the structural parameters collated in Table 1.

Taking into account the bilayer structure presented in Table 1 to describe the Mg/Co/Sc/Co multilayer, we simulate the x-ray standing wave curves of the Co L and Mg K emissions, as shown in figures 9(a) and (b) respectively. It can be seen that the simulations reproduce well the general shape and the angle of the standing wave feature of the experimental curves in both ranges. However, the agreement is not perfect. Thus, simulations were also done with two other sets of structural parameters, which give good fits of the reflectivity curves in both hard and soft x-ray ranges. In these two structures, the first period of the stack is oxidized and mixed as for the bilayer structure, see Table 1. The other 39 periodic repetitions of the stack are made of a quadrilayer, Co/Sc/Co/Mg, or an hexalayer, Co/Sc_3Co/Sc/Sc_3Co/Co/Mg where the thin Sc_3Co layers, thickness less than 1 nm, are introduced to take into account a partial mixing of the Sc and Co layers. We also present in figure 9 the simulations obtained with the quadrilayer, but not those obtained with the hexalayer as they do not reproduce the standing wave curves. For each of the Co and Sc layers obtained with the quadrilayer model, their fitted thickness and roughness of are quite close: Co top, thickness 0.6 nm, roughness 0.7 nm; Sc, thickness 2.2 nm, roughness 1.1 nm; Co bottom, thickness 0.5 nm, roughness 0.4 nm. This indicates a mixing or interdiffusion between the Sc and Co layers.

Figure 9: Experimental x-ray standing wave curves of the Co L (a) and Mg K (b) emissions from the Mg/Co/Sc/Co sample (solid red line) compared to simulated curves obtained from a bilayer structure with structural parameters give in Table 1 (dotted blue line) and from a quadrilayer structure (dashed green line).

When comparing the simulations made with the bilayer and quadrilayer structures, it is observed that the position of and shape of the standing wave feature (around 4.5°) is almost the same in both models. However, the bilayer structure leads to a simulated curve closer to the experimental one regarding the shape of the background in the 2 – 4° angular range of the Co L curve, figure 9(a), and the position of the total reflection feature at 1.6° of the Mg K curve, figure 9(b). Thus, the bilayer model suggested by the electron microscopy images and elemental profiles is the best suited to reproduce at the same time the reflectivity and standing wave curves. One could think that the agreement between experimental curves and simulations could be improved by changing the description of the stack, for example, by introducing some supplementary interfacial layers, or changing the composition of the scandium oxide, or considering a small departure from the bulk densities for the B_4C, Mg and Co layers. However, at this stage it does not seem relevant do develop more complicated models to describe the quadri-layer stack. Indeed, this would lead to only incremental improvements of the fits of the reflectivity curves and regarding the standing wave curves there is too much uncertainty on the optical indices of Co and Mg in the Co L and Mg K absorption edges respectively. Moreover the sine function used to take into account the geometry effect is probably too simplistic. Thus even with a more sophisticated description of the stack, we are not sure to clearly improve the comparison between the experimental and simulated standing wave curves.

Conclusion

Sc/Mg, Sc/Co/Mg and Sc/Co/Mg/Co periodic multilayers have been characterized by hard and soft x-ray reflectivity, x-ray fluorescence in x-ray standing wave mode and transmission electron microscopy on cross sections. The two-layer system has very poor reflective properties as some strong intermixing takes place between the Sc and Mg layers, destroying the optical contrast between layers required for obtaining a good reflectance. The tri-layers and quadri-layer are also subjected to an intermixing, but between the Sc and Co layers. This results in the transformation of the three Co/Sc/Co layers in a single ScCo layer with asymmetric sides and thus in the formation of ScCo/Mg bilayers. As the Mg layers remain free of Sc and Co atoms, a good contrast exists between Mg and ScCo layers, providing good reflective properties.

The quadri-layer can be a useful dispersive element for x-ray spectroscopy in the nitrogen K range as its reflectance simulation performed with the structure determined here lead to a reflectance of 32% and a bandwidth of 5 eV. It can be anticipated that a Sc/Mg quadri-layer with Cr, Zr or Nb as diffusion barriers would have improved properties. Indeed, in this case, the mixing enthalpies between all elements is positive [22]. This would prevent the interdiffusion between the various layers and help to keep well-defined interfaces and thus high reflectance.

About two years after the preparation of the Sc/Co/Mg/Co quadri-layer, which was stored in air, a strong change on the reflectivity curve obtained in the hard x-ray range. This leads to an increase of the multilayer period and a doubling of the Bragg peaks, demonstrating a large evolution in the structure of the stack. This has been ascribed to the oxidation of the multilayer owing to the great affinity of scandium and magnesium with oxygen. Nonetheless,

in general, crystals and multilayers are kept in vacuum in crystal spectrometers. Thus, we think that the proposed Sc/Co/Mg/Co multilayer can be useful as a dispersive element.

Acknowledgments

All experiments related to transmission electron microscopy were performed at the IMPMC microscopy platform at Sorbonne Université. Igor A. Makotkhin and Cedric P. Hendrikx from University of Twente are thanked for fruitful discussions.

References

[1] D. Attwood, *Soft X-Rays and Extreme Ultraviolet Radiation* (Cambridge University Press, 2000).
[2] P. Jonnard and C. Bonnelle, X-Ray Spectrom. **40**, 12 (2011).
[3] F. Schäfers, H.-C. Mertins, F. Schmolla, I. Packe, N.N. Salashchenko, and E.A. Shamov, Appl. Opt. **37**, 719 (1998).
[4] M. Wu, C. Burcklen, J.-M. André, K. Le Guen, A. Giglia, K. Koshmak, S. Nannarone, F. Bridou, E. Meltchakov, S. de Rossi, F. Deltte, and P. Jonnard, Opt. Eng. **56**, 117101 (2017).
[5] M. Prasciolu, A.F.G. Leontowich, K.R. Beyerlein, and S. Bajt, Appl. Opt. **53**, 2126 (2014).
[6] Q. Huang, J. Fei, Y. Liu, P. Li, M. Wen, C. Xie, P. Jonnard, A. Giglia, Z. Zhang, K. Wang, and Z. Wang, Opt. Lett. **41**, 701 (2016).
[7] Q. Yi, Q. Huang, J. Zhang, X. Wang, R. Qi, Z. Zhang, R. Xu, T. Peng, P. Jonnard, A. Giglia, and Z. Wang, Vacuum **146**, 187 (2017).
[8] Q. Huang, Q. Yi, Z. Cao, R. Qi, R.A. Loch, P. Jonnard, M. Wu, A. Giglia, W. Li, E. Louis, F. Bijkerk, Z. Zhang, and Z. Wang, Sci. Rep. **7**, 12929 (2017).
[9] Le.V. Azaroff, *X-Ray Spectroscopy*, McGraw-Hill, Inc. (New York, 1974).
[10] *X-Ray Spectrometry: Recent Technological Advances*, John Wiley & Sons, Ltd (Kouichi Tsuji, Jasna Injuk, René van Grieken, Chichester, 2004).
[11] C. Hombourger, P. Jonnard, J.-M. André, and J.-P. Chauvineau, X‐Ray Spectrom. **28**, 163 (1999).
[12] J.-M. André, P. Jonnard, C. Michaelsen, J. Wiesmann, F. Bridou, M.-F. Ravet, A. Jérome, F. Delmotte, and E.O. Filatova, X‐Ray Spectrom. **34**, 203 (2005).
[13] K. Le Guen, H. Maury, J.-M. André, P. Jonnard, A. Hardouin, F. Delmotte, and M.-F. Ravet-Krill, Appl. Phys. Lett. **91**, 234104 (2007).
[14] K. Le Guen, M.-H. Hu, J.-M. André, P. Jonnard, S.K. Zhou, H.C. Li, J.T. Zhu, Z.S. Wang, and C. Meny, J. Phys. Chem. C **114**, 6484 (2010).
[15] J. Zegenhagen and A. Kazimirov, *The X-Ray Standing Wave Technique: Principles and Applications* (World Scientific, 2013).
[16] Y. Tu, Y. Yuan, K. Le Guen, J.-M. André, J. Zhu, Z. Wang, F. Bridou, A. Giglia, and P. Jonnard, J. Synchrotron Radiat. **22**, 1419 (2015).
[17] S. Nannarone, F. Borgatti, A. DeLuisa, B.P. Doyle, G.C. Gazzadi, A. Giglia, P. Finetti, N. Mahne, L. Pasquali, M. Pedio, G. Selvaggi, G. Naletto, M.G. Pelizzo, and G. Tondello, AIP Conf. Proc. **705**, 450 (2004).
[18] D.L. Windt, Comput. Phys. **12**, 360 (1998).
[19] J.-P. Chauvineau and F. Bridou, J. Phys. IV **06**, C7 (1996).
[20] P. Jonnard, Y.-Y. Yuan, K. Le Guen, J.-M. André, J.-T. Zhu, Z.-S. Wang, and F. Bridou, J. Phys. B At. Mol. Opt. Phys. **47**, 165601 (2014).

[21] W. Li, J. Zhu, X. Ma, H. Li, H. Wang, K.J.S. Sawhney, and Z. Wang, Rev. Sci. Instrum. **83**, 053114 (2012).
[22] A. Debski, R. Debski, and W. Gasior, Arch. Metall. Mater. **59**, 1337 (2014).
[23] H. Okamoto, J. Phase Equilibria Diffus. **31**, 85 (2010).

AIP Publishing

Journal of Applied Physics

PLEASE CITE THIS ARTICLE AS DOI: 10.1063/1.5128867

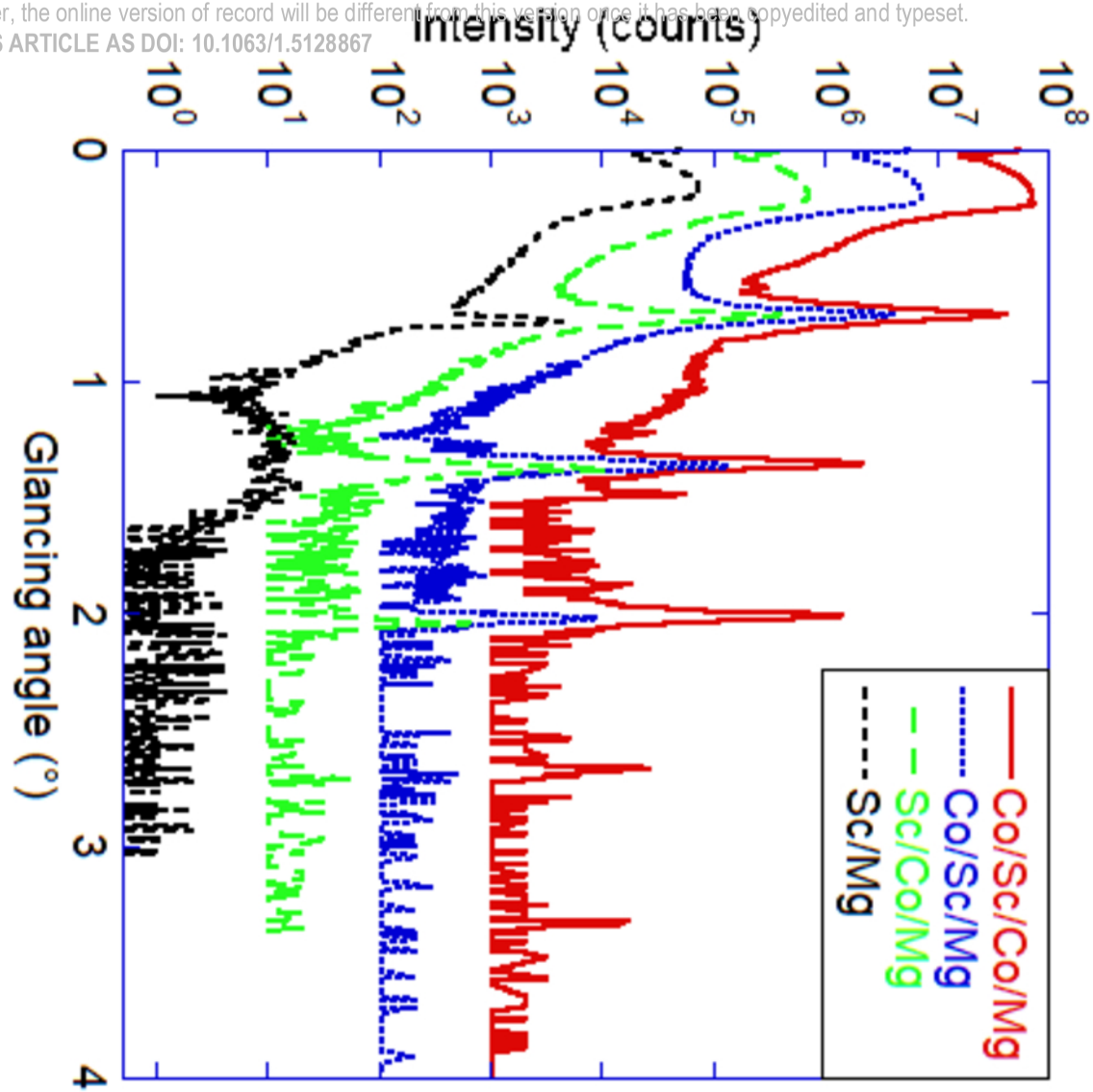

PLEASE CITE THIS ARTICLE AS DOI: 10.1063/1.5128867

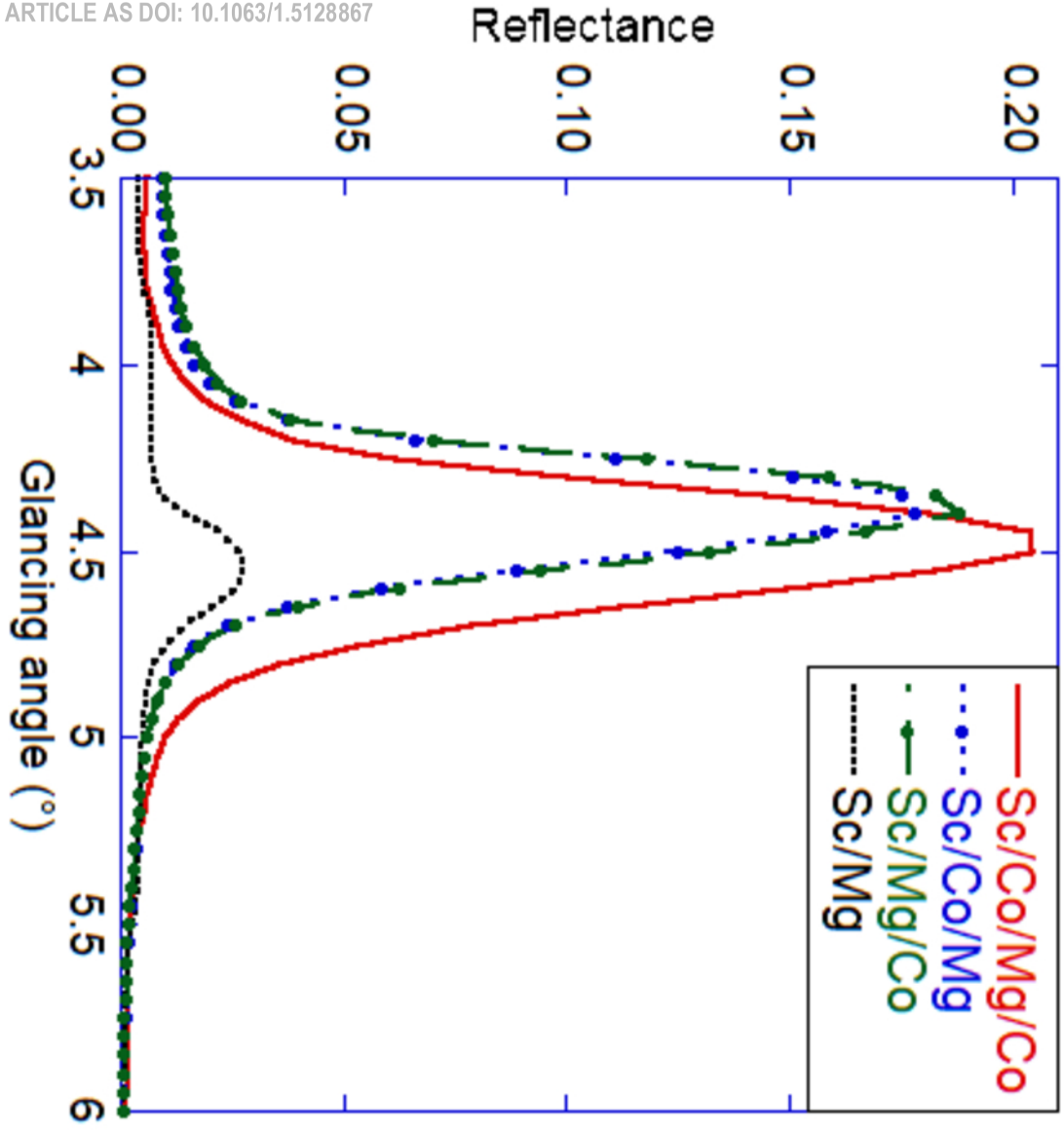

AIP Publishing

Journal of Applied Physics

ACCEPTED MANUSCRIPT

PLEASE CITE THIS ARTICLE AS DOI: 10.1063/1.5128887

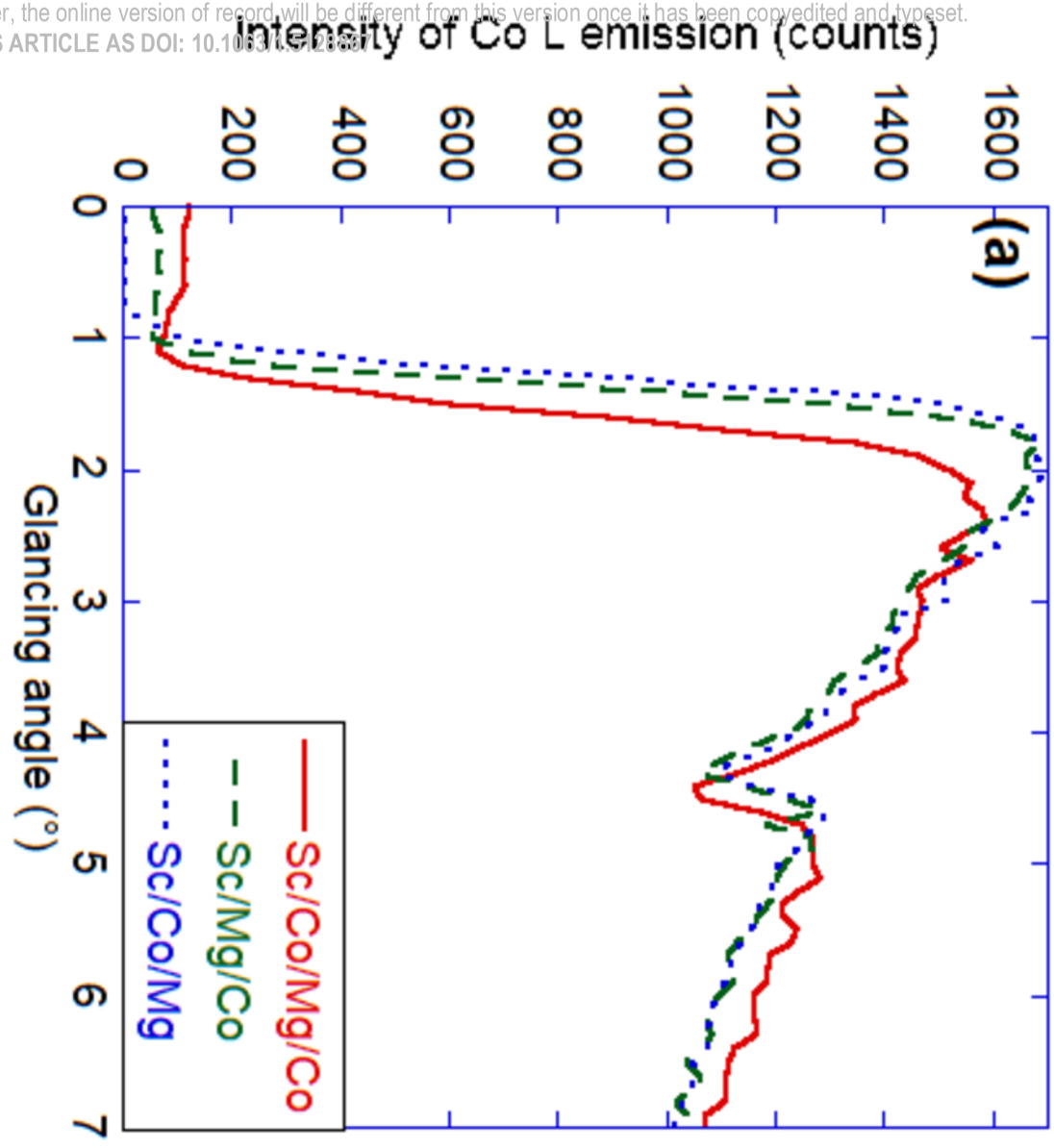

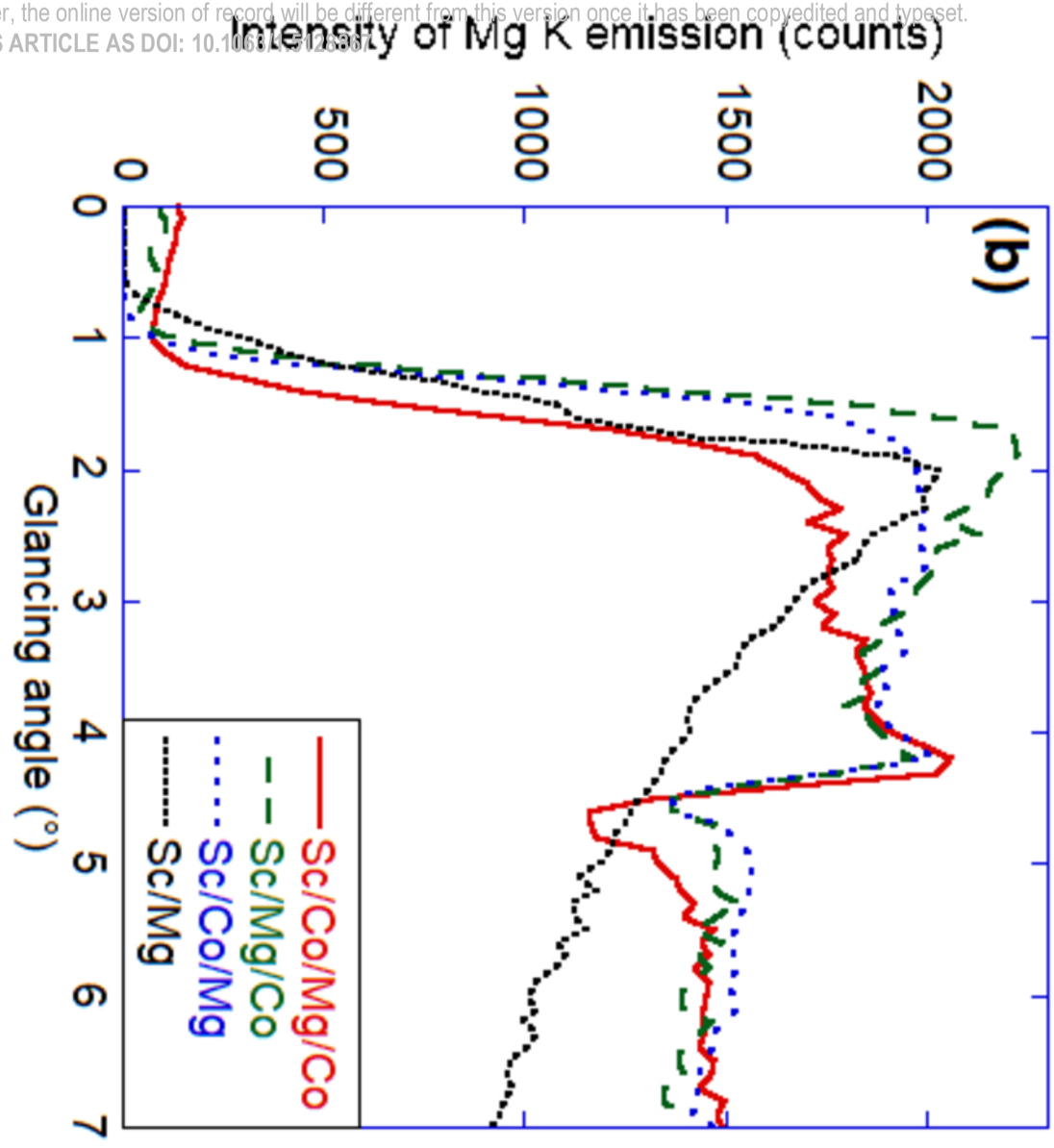

AIP Publishing

Journal of Applied Physics

ACCEPTED MANUSCRIPT

This is the author's peer reviewed, accepted manuscript. However, the online version of record will be different from this version once it has been copyedited and typeset.
PLEASE CITE THIS ARTICLE AS DOI: 10.1063/1.5128867

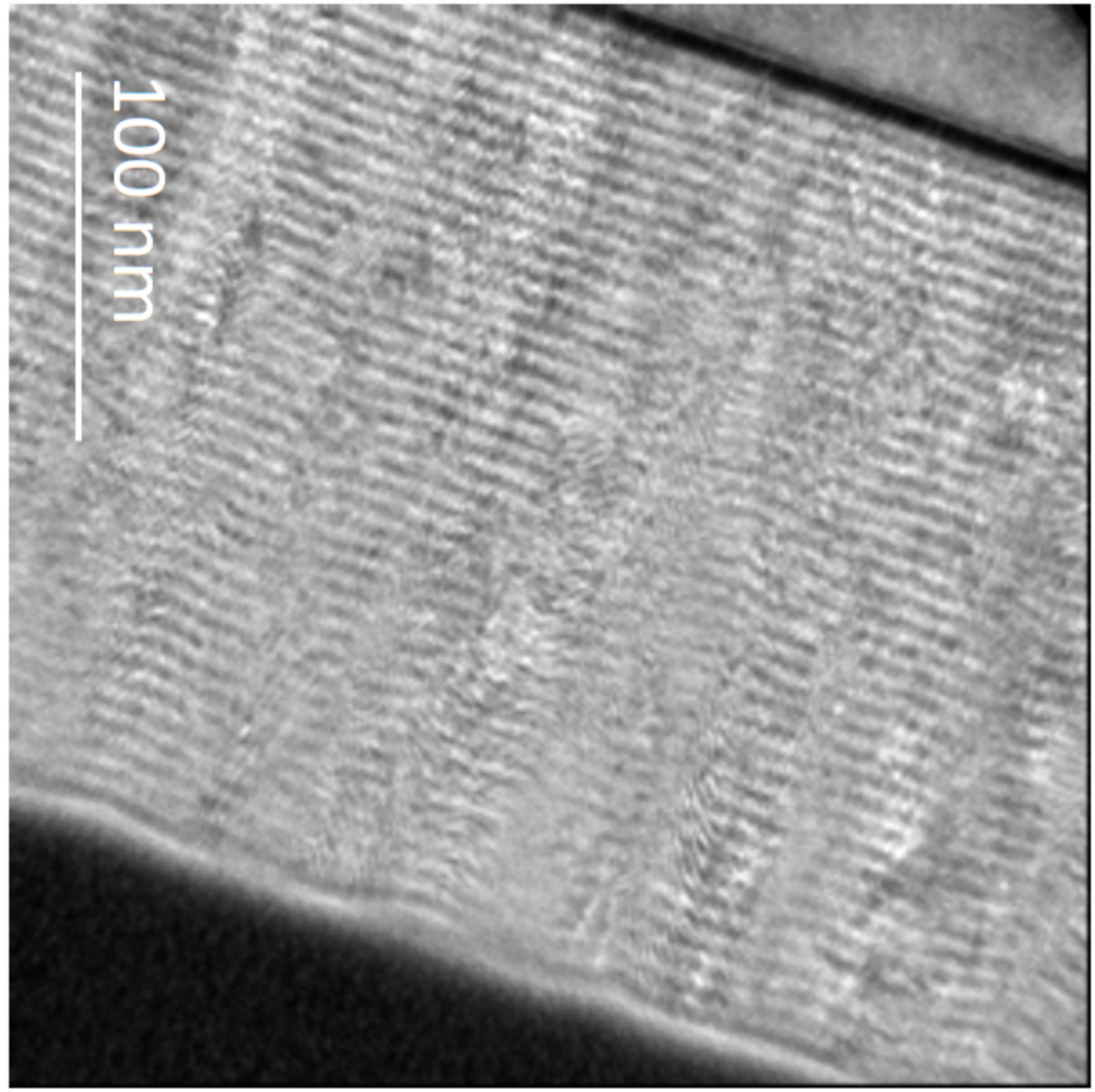

AIP Publishing

Journal of Applied Physics

ACCEPTED MANUSCRIPT

This is the author's peer reviewed, accepted manuscript. However, the online version of record will be different from this version once it has been copyedited and typeset.
PLEASE CITE THIS ARTICLE AS DOI: 10.1063/1.5128867

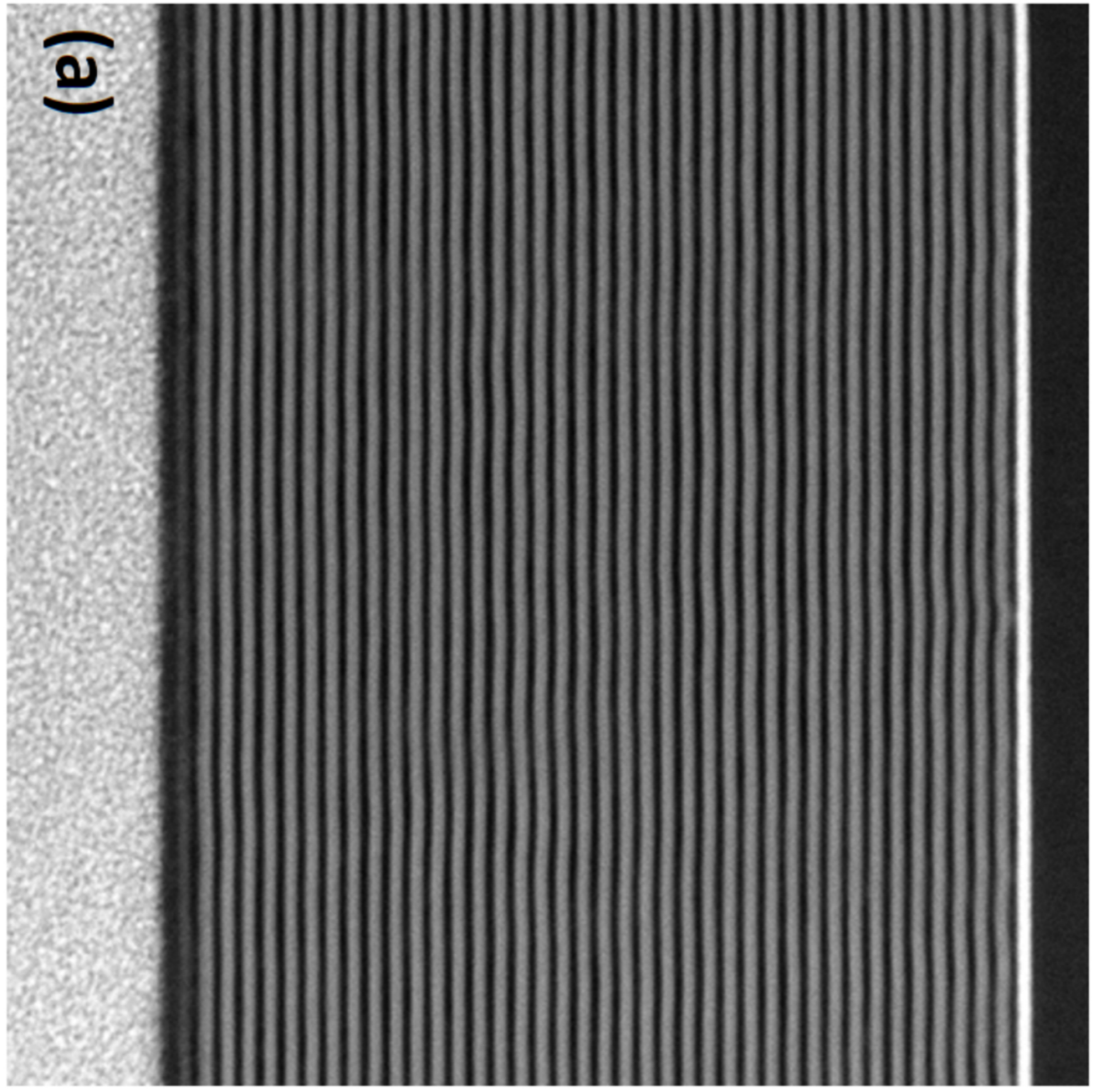

AIP Publishing

Journal of Applied Physics

ACCEPTED MANUSCRIPT

This is the author's peer reviewed, accepted manuscript. However, the online version of record will be different from this version once it has been copyedited and typeset.
PLEASE CITE THIS ARTICLE AS DOI: 10.1063/1.5128867

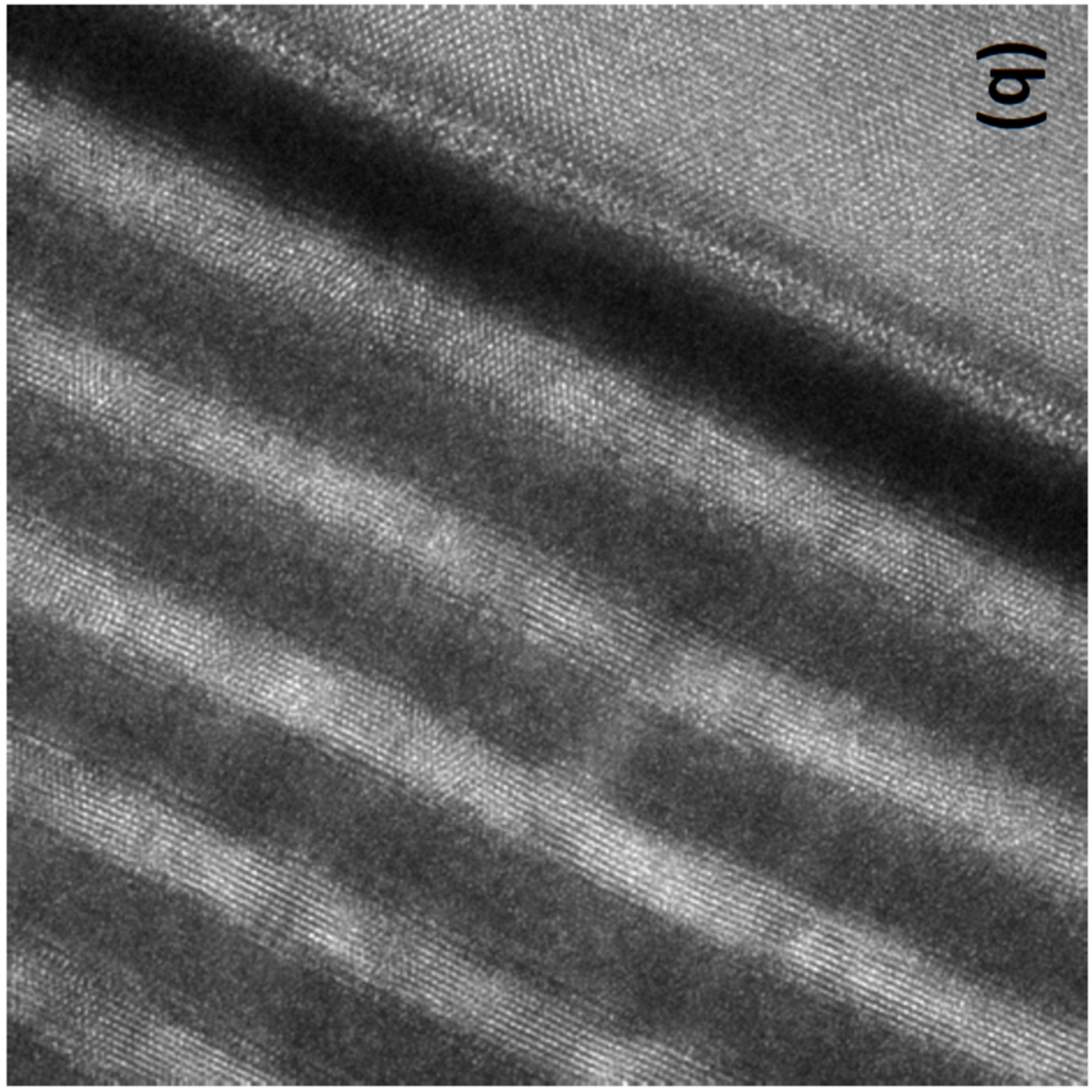

Journal of Applied Physics

AIP Publishing

Journal of Applied Physics

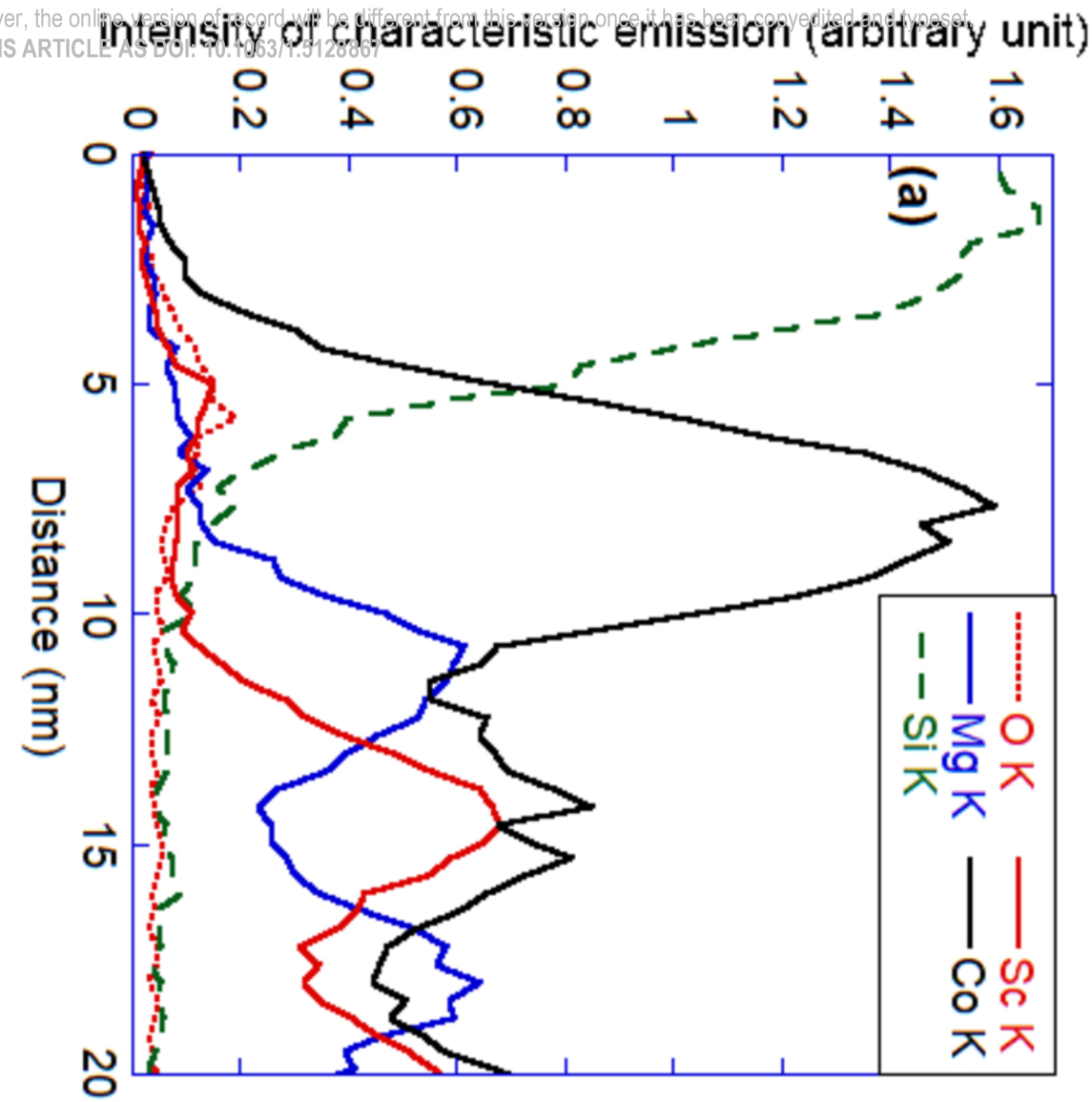

AIP Publishing

Journal of Applied Physics

ACCEPTED MANUSCRIPT

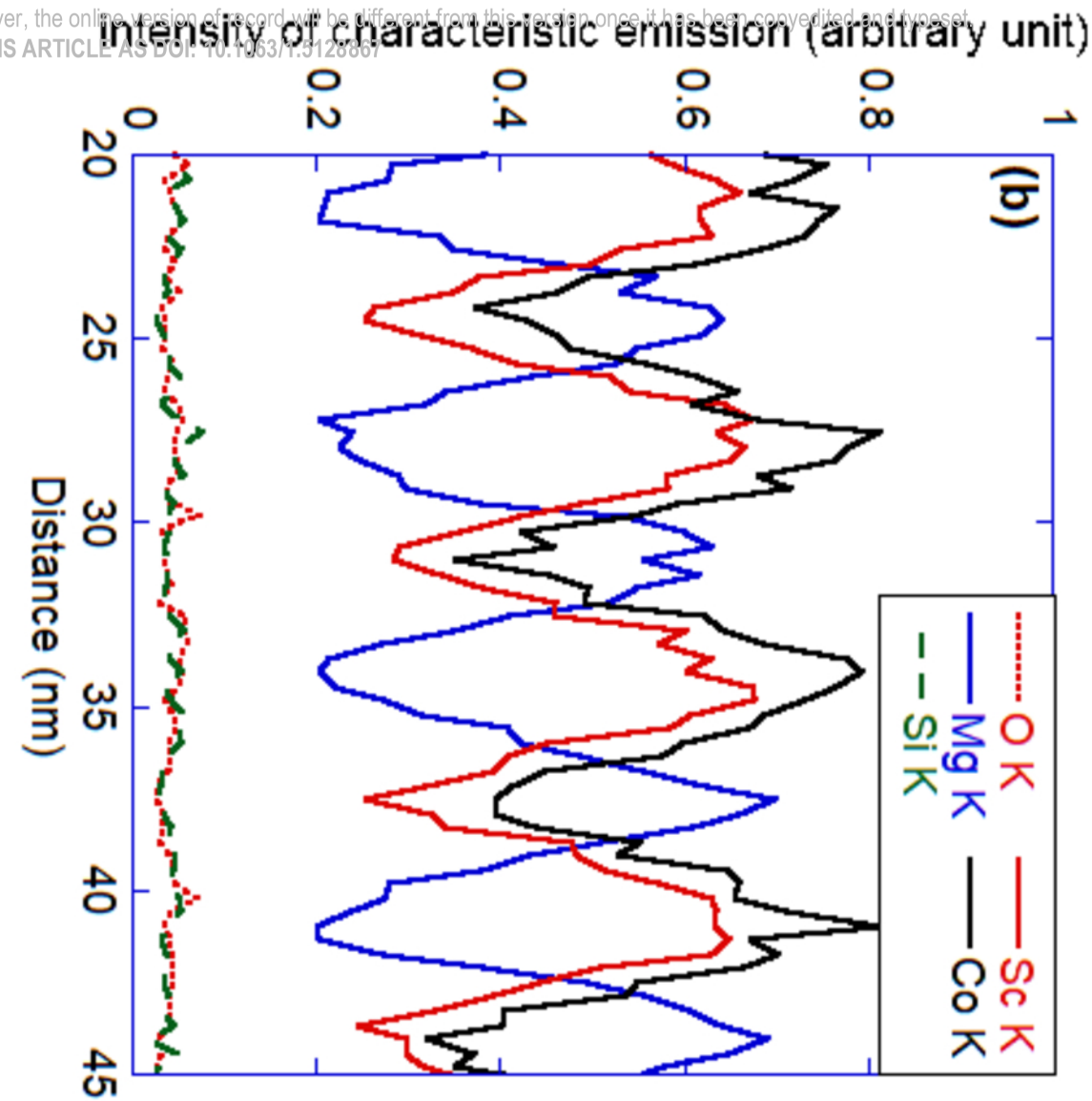

AIP Publishing

Journal of Applied Physics

ACCEPTED MANUSCRIPT

PLEASE CITE THIS ARTICLE AS DOI: 10.1063/1.5128867

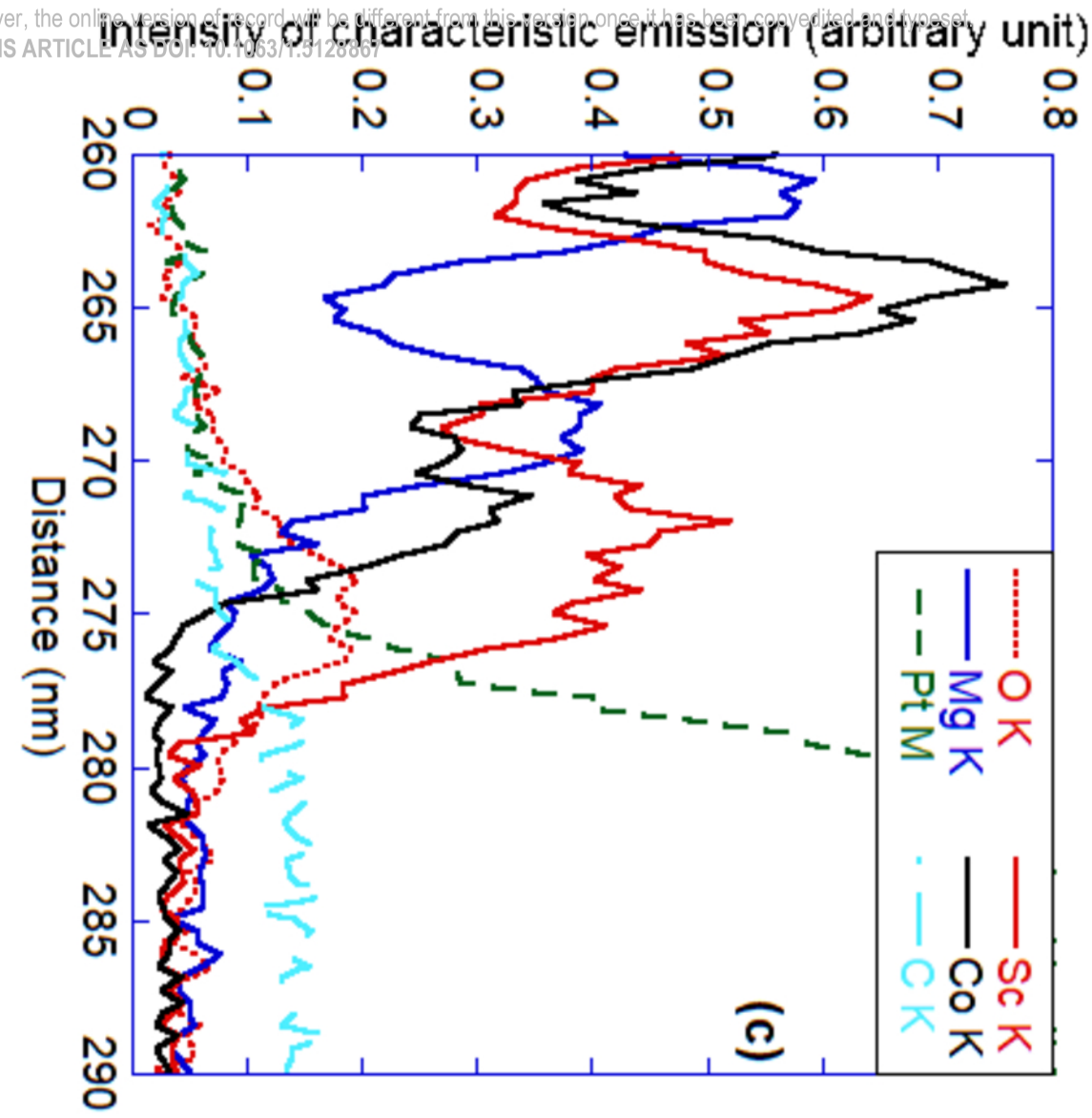

AIP Publishing
Journal of Applied Physics

PLEASE CITE THIS ARTICLE AS DOI: 10.1063/1.5128867

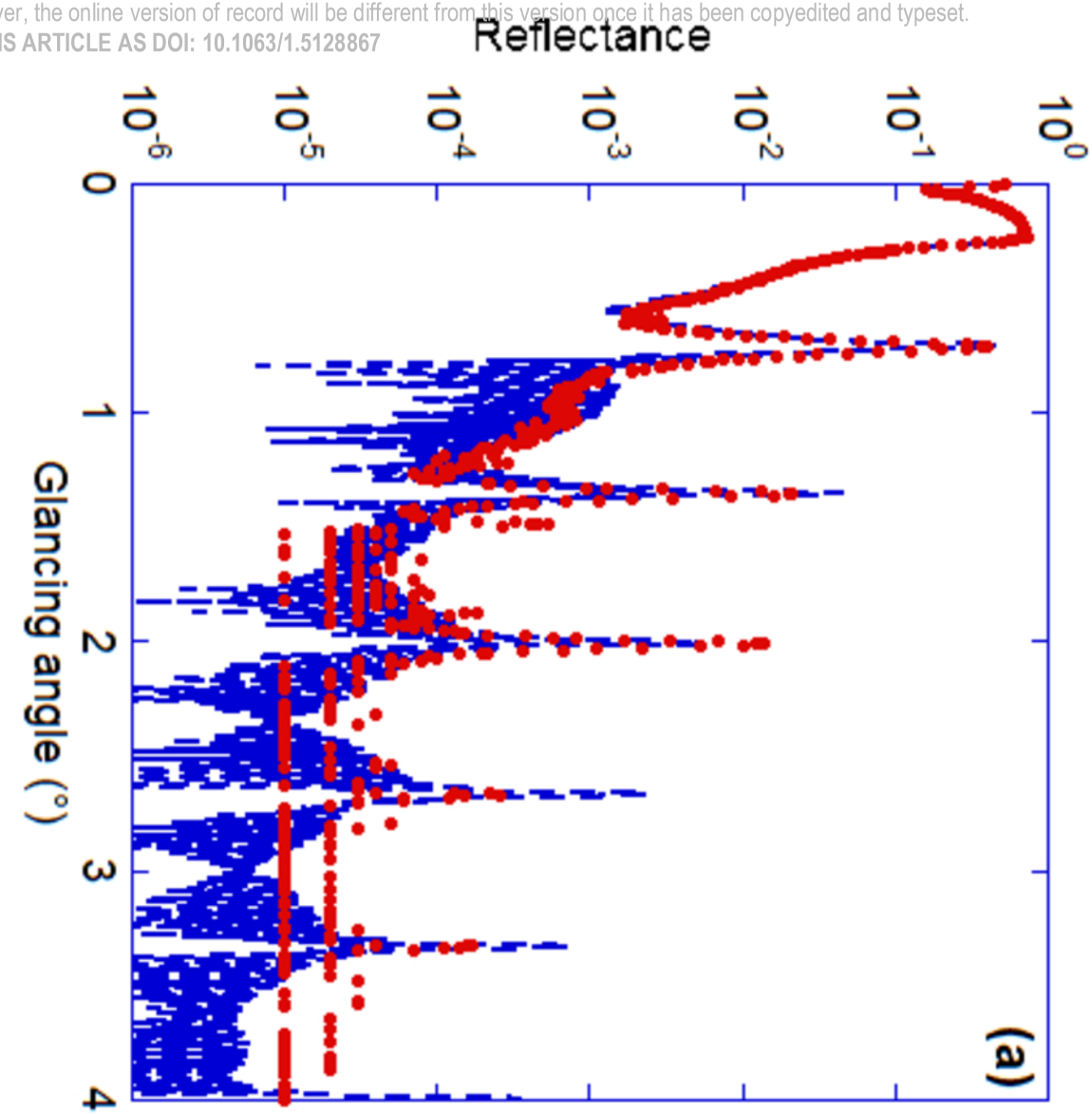

AIP Publishing
Journal of Applied Physics
ACCEPTED MANUSCRIPT

PLEASE CITE THIS ARTICLE AS DOI: 10.1063/1.5128867

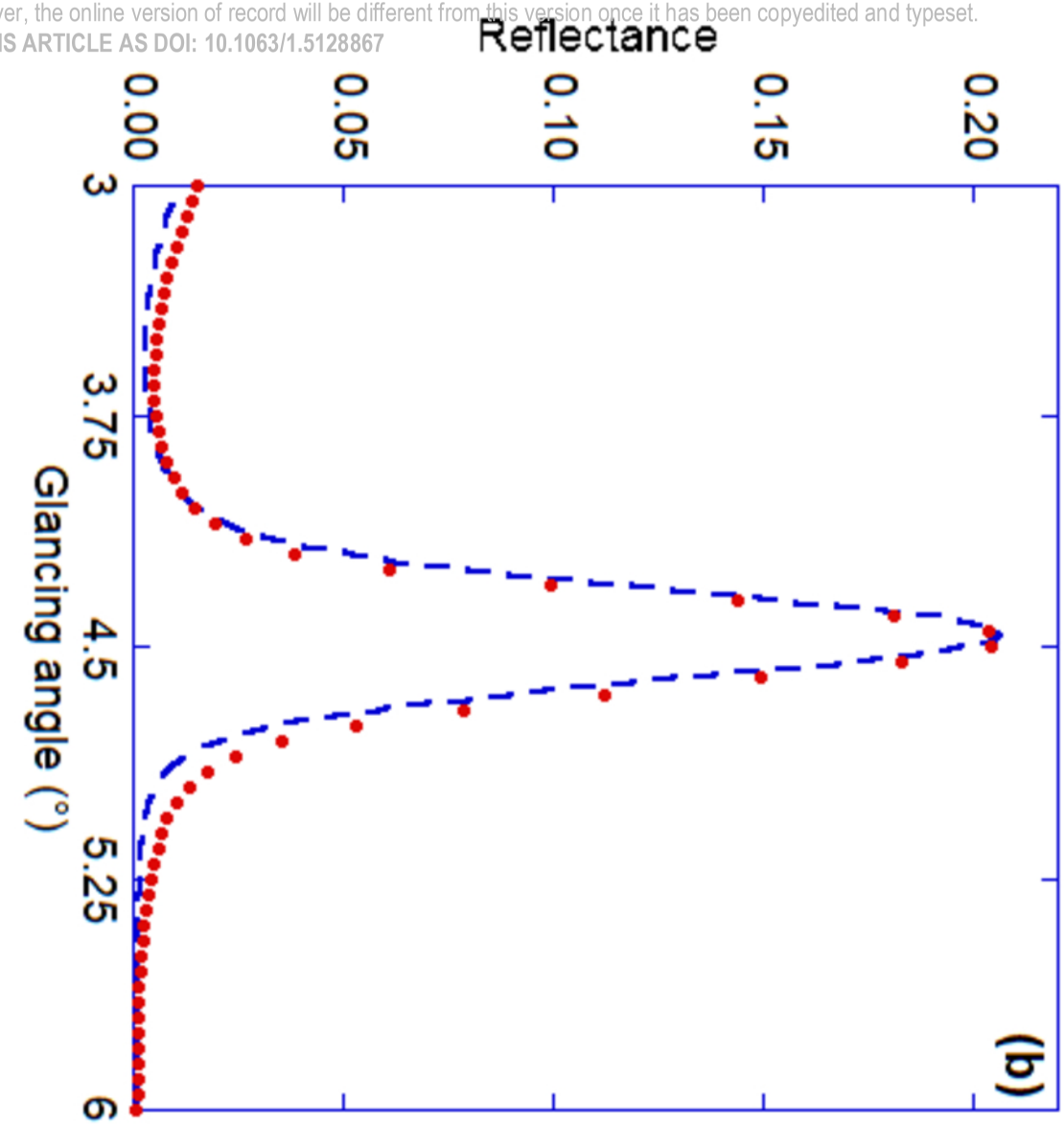

AIP Publishing

Journal of Applied Physics

ACCEPTED MANUSCRIPT

PLEASE CITE THIS ARTICLE AS DOI: 10.1063/1.5128867

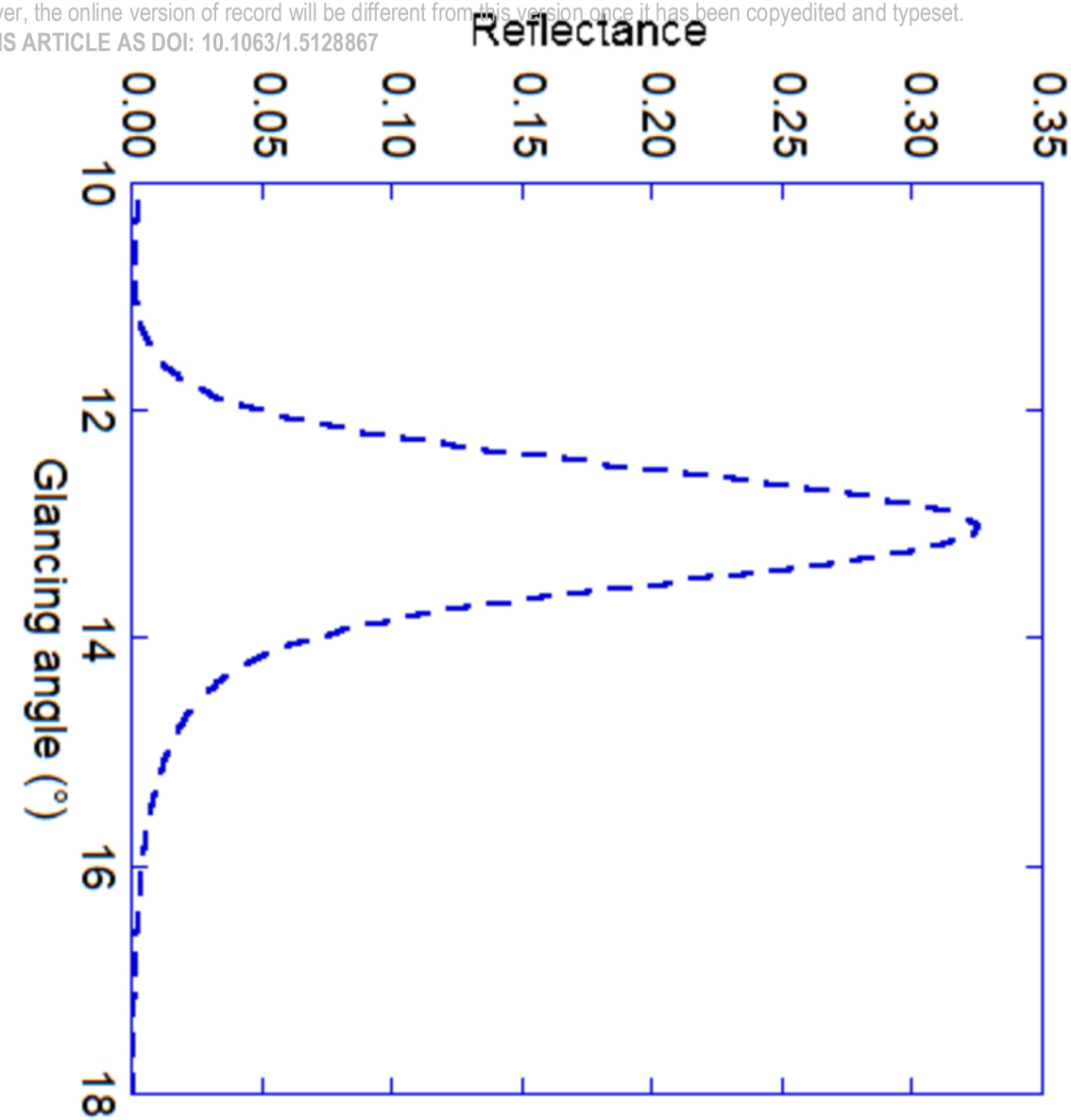

AIP Publishing

Journal of Applied Physics

ACCEPTED MANUSCRIPT

PLEASE CITE THIS ARTICLE AS DOI: 10.1063/1.5128867